Interfacial Characterization of Dentin Conditioned with Chitosan Hydroxyapatite Precursor Nanocomplexes Using Time-of-flight Secondary Ion Mass Spectrometry

Anam Hashmi, BDS, MSc,[*] Rana N.S. Sodhi, PhD,[†] and Anil Kishen, BDS, MDS, PhD[‡]*

ABSTRACT

Introduction: The purpose of this study was to evaluate the effect of chitosan-hydroxyapatite precursor (C-HA) nanocomplex conditioning on the chemical modifications at the tricalcium silicate sealer-dentin interface using time-of-flight secondary ion mass spectrometry. **Methods:** Dentin slabs from human premolar root dentin were prepared, demineralized, and randomly distributed between control and C-HA nanocomplex conditioned groups. Tricalcium silicate sealer was applied, and the slabs were allowed to set in 100% humidity for 10 days. The cross-sectional area was exposed, and the sealer-dentin interface was characterized for chemical/ultrastructural evaluation with time-of-flight secondary ion mass spectrometry and transmission electron microscopy, respectively. **Results:** Chemical analysis revealed the presence of an ion-rich layer constituted of abundant phosphates (PO_2^-, PO_3^-, and PO_4^-), hydroxide (OH^-), and chitosan fragments ($C_2H_4NO^-$, $C_3H_4NO_2^-$, $C_2H_5O_2^+$, $C_2H_6NO^+$, $C_4H_6NO_2^+$, $C_5H_6NO^+$, and $C_5H_5O_2^+$) on the dentin surface at the sealer-dentin interface and subsurface dentin after conditioning with C-HA nanocomplexes. In contrast, a decreased interfacial presence of calcium (Ca^+) and calcium phosphates ($CaPO_2^+$, $CaPO_3^+$, $CaPO_4^+$, and $Ca_2PO_3^+$) and the absence of phosphate fragments in the control were noted. Ultrastructural evaluation showed an interfacial layer (<1 μm) with interrupted mineral aggregates in the controls as opposed to a continuous (5 μm) mineral layer formation on the conditioned dentin. **Conclusions:** C-HA nanocomplex conditioning of dentin before tricalcium silicate sealer application resulted in a chemically modified dentin substrate with an ion-rich layer consisting of phosphate, calcium, calcium phosphates, and chitosan that chemically modified the dentin surface/subsurface. *(J Endod 2019;45:1513–1521.)*

SIGNIFICANCE

Dentin substrate conditioning with C-HA nanocomplexes may find potential application in enhancing the chemical interaction of sealers with dentin for the reinforcement of interfacial integrity.

KEY WORDS

Chitosan; dentin conditioning; interface; nanocomplexes; sealer-dentin interface

Dentin is a biocomposite composed of carbonated hydroxyapatite mineral crystallites, type I collagen fibrils, and noncollagenous macromolecules spanning over several length scales[1]. However, iatrogenic application of chemicals and/or medications during root canal therapy induces ultrastructural and compositional alterations in dentin that affect its physicochemical and mechanical characteristics[2,3]. The use of EDTA and sodium hypochlorite on dentin as commonly used root canal irrigants results in surface/subsurface demineralization and irreversible, nonspecific dissolution of the organic constituents[4]. The mineral denuded collagen shows poor surface polarity and poses challenging substrate for remineralization[5]. The endodontic chemical may also compromise the surface wettability, which further limits the extent of interaction between the root canal sealer and dentin at the interface[3,6]. Furthermore, dentin possesses an anastomosing network of secondary dentinal tubules that encourages fluid movement and contaminant ingress even when frank interfacial gaps are lacking[7]. All of these factors

From the *Kishen Lab, Faculty of Dentistry and †Ontario Centre for the Characterization of Advanced Materials, Department of Chemical Engineering and Applied Chemistry, University of Toronto, Ontario, Canada; and ‡Department of Dentistry, Mount Sinai Health System, Mount Sinai Hospital, Toronto, Ontario, Canada

Address requests for reprints to Dr Anil Kishen, Faculty of Dentistry, University of Toronto, Toronto M5G 1G6, Canada. E-mail address: anil.kishen@utoronto.ca
0099-2399/$ - see front matter

https://doi.org/10.1016/j.joen.2019.08.011

facilitate progressive collagen degradation and increased fracture predilection in root-filled teeth with time[8].

Tricalcium silicate–based materials (TCSs) are hydraulic in nature and interact with dentin through carbonated apatite formation on contact with physiological fluids[9,10]. Therefore, the physicochemical profile of dentin plays a crucial role in directing the mechanics of this interaction and subsequent mineral formation[5,11]. Differences in the nature of precipitate formation in the bulk of TCSs and that formed at the sealer-dentin interface have been reported, chiefly because of the inadequacy and lack of accessibility of phosphorous ions[12]. The availability of a sustained mineral source and subsequent nucleation on a hydrophobic, mineral denuded collagen surface are current challenges in dentin remineralization[5]. However, to the best of our knowledge, no studies have characterized the TCS sealer–dentin interface or developed strategies to improve the sealer-dentin interfacial integrity via concepts of dentin remineralization. In this line, polymer-based guided tissue mineralization using chitosan-hydroxyapatite precursor (C-HA) nanocomplexes may serve as an effective strategy.

Chitosan is an abundant biopolymer consisting of β-(1-4) glucosamine units[13]. Chitosan and its derivatives have been found to offer different advantages because of their biocompatible, bioactive, and antibacterial nature[13]. C-HA nanocomplexes are an organic-inorganic composite that are functionally inspired by the role of noncollagenous proteins. Their bioactivity is facilitated through a dense polyanionic surface charge (−27 mV)[14] on the water-soluble chitosan backbone that allows sequestration and stabilization of hydroxyapatite precursor phases (amorphous calcium phosphate) with its carboxyl groups[14]. This facilitates synergistic intra- and extrafibrillar collagen mineralization to take place[15,16], similar to how it occurs in biomineralization. Dentin conditioning with C-HA nanocomplexes has been reported to promote TCS sealer–dentin interaction through increased surface wettability, greater sealer penetration into the dentinal tubules, and enhanced ultimate tensile strength of endodontic irrigant–treated dentin[14].

Time-of-flight secondary ion mass spectrometry (TOF-SIMS) is a well-established technique in material sciences that allows analysis and identification of both organic and inorganic fractions such as hydroxyapatite with millimass precision and monolayer sensitivity[17]. It provides high-resolution mass spectra along with their spatial ion maps[18–20]. Recently, TOF-SIMS analysis has been used to study precipitate formation on the dentin surface and in dentinal tubules subsequent to the application of different irrigants[21]. Although there is a lack of knowledge on how dentin surface chemistry affects the interfacial characteristics of TCS sealers, TOF-SIMS, because of its inherent advantages, would be an ideal method to characterize the sealer-dentin interface. The aim of the current study was to chemically characterize the TCS sealer–dentin interface after prior dentin conditioning with C-HA nanocomplexes.

MATERIALS AND METHODS

Five extracted human premolar teeth were collected under the university ethical guidelines (protocol identification number: 35073) and stored in 0.9% saline until use. Slabs of root dentin were prepared by sectioning the root along the long axis of the tooth using a diamond wafering blade (4 × 0.12 × $^1/_2$ inches [Precision Smart Cut; UKAM Industrial Superhard Tools, Valencia, CA]) mounted on a slow-speed saw (Isomet Low Speed Saw; Buehler, Lake Bluff, IL) under running water. Each slab (n = 6) was then shaped and grinded with carbide paper discs to final dimensions of 6 × 4 × 0.2 mm. Slabs were demineralized (17% EDTA for 7 days), ultrasonicated (10 minutes with deionized water), and randomly distributed between the control and C-HA nanocomplex conditioned group.

Carboxymethyl chitosan was synthesized according to an earlier protocol[22]. Amorphous calcium phosphate was then grafted by the addition of K_2HPO_4 and $CaCl_2$[12]. The resultant gel was freeze-dried and processed to a powder[16]. Fresh slurry of C-HA nanocomplexes was prepared by dissolving 2 mg C-HA nanocomplex powder in deionized water. Demineralized dentin slabs were conditioned in 1 mL of a 2-mg/mL solution of C-HA nanocomplexes for 30 minutes followed by sealer application in the test group. Demineralized slabs in the control group remained unexposed to conditioning treatment before sealer application. In each group, sealer (iRoot SP; Innovative BioCreamix Inc, Vancouver, Canada) was allowed to spread into a uniform thickness layer in between 2 dentin slabs that were sandwiched under weight and incubated in 100% humidity at 37°C with 5% CO_2 for a 10-day period. The samples were stabilized on a customized, polystyrene jig; secured in a mount; and sectioned to expose the sealer-dentin interface using a microtome (Leica EM UC6/FC6 Ultra-cryomicrotome; Leica Microsystems GmbH, Wetzlar, Germany). One sample from each group was processed for ultrastructural analysis with transmission electron microscopy.

TOF-SIMS Analysis

Dentin surface analysis was performed by TOF-SIMS (TOF-SIMS V; IONTOF GmbH, Münster, Germany). A Bi_3^{++} cluster primary ion source was used with a bismuth liquid metal ion gun operated in a high mass resolution bunched mode over an area of 500 × 500 μm for 100 seconds. Additionally, a high spatial resolution imaging mode ("burst alignment") was used to obtain spectral images (256 × 256 pixels) from 20 scans over an area of 150 × 150 μm. A pulsed electron flood gun was used for charge neutralization. The calibration of the mass scale was performed using standard, identifiable, and well-spaced peaks found in all the spectra. Both positive and negative polarity mass spectra and spatial chemical maps for molecular fragments of interest were generated through regions of interest (ROIs) at the interface (5 × 25um) and total dentin (150 × 70 μm). Individually run C-HA nanocomplex powder, set TCS sealer, and demineralized dentin were used as reference samples in order to select characteristic fragments. Spectral comparisons were performed after normalization of the intensity, proportionally to the total intensity of each spectrum[23]. Thus, data from both normalized spectral intensities and spectral chemical maps are presented later.

Transmission Electron Microscopic Evaluation

Specimens were fixed with Karnovsky fixative (2.5 wt% glutaraldehyde buffered to pH = 7.3) for 3 days at 4°C and postfixed in 1% osmium tetroxide for 1 hour. The specimens were dehydrated in an ascending ethanol series (30%–100%), immersed in propylene oxide as a transition medium, and ultimately embedded in pure epoxy resin. Ninety-nanometer-thick sections were prepared. Sections containing the material-dentin interface were stained with 2% aqueous uranyl acetate and Reynolds' lead citrate. The sections were examined along the cross section using a JEM-1230 transmission electron microscope (JEOL, Tokyo, Japan) at 110 kV.

RESULTS

TOF-SIMS Analysis

Total ion and CN^- maps are shown in Figure 1*A–D*. A distinguishable interfacial zone (5 μm) because of differences in pixel intensity is seen lacking in the control (Fig. 1*A*) in comparison with the conditioned dentin

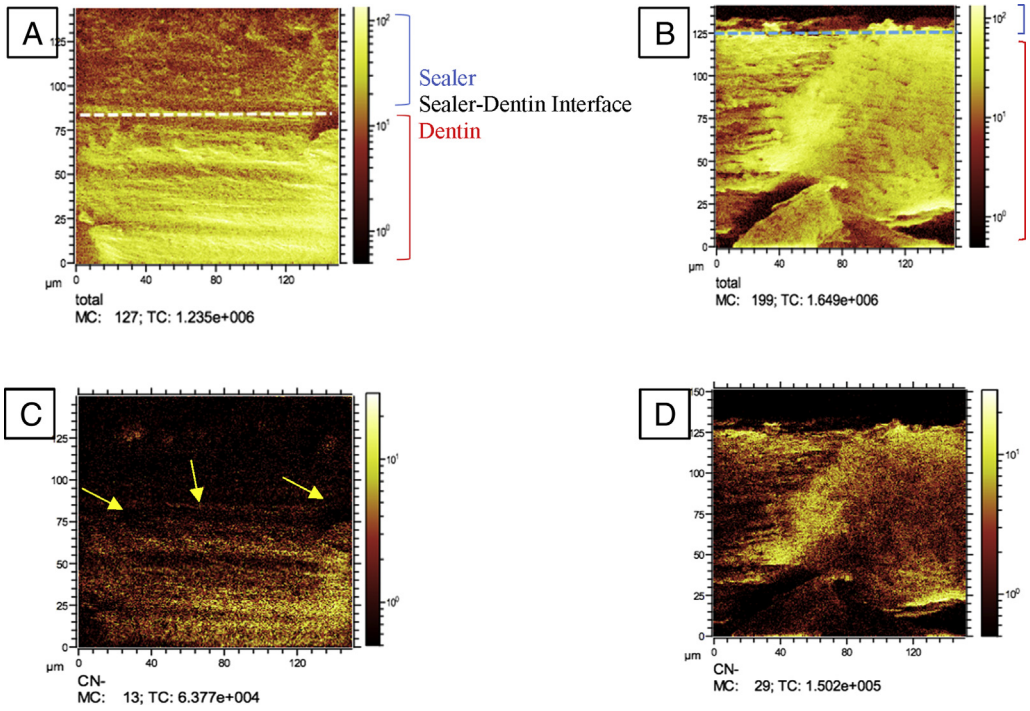

FIGURE 1 – Total ion maps for the (*A*) control and (*B*) C-HA nanocomplex conditioned dentin. The interfacial layer with differences in pixel intensity can be seen (*dashed line* marks the interfacial boundary). (*C*) The CN^- chemical ion map of the control sample showing no signal zones (*yellow arrows*) suggestive of degraded collagen. (*D*) Intense CN^- signals of integrated C-HA nanocomplexes at the interface/subsurface in the conditioned dentin. (*E* and *F*) Red-green overlays of the organic fragment (C_2H_4NO [*red*]) with phosphates (PO_2^-, PO_3^-, and PO_4^- [*green*]). (*E*) A minimal presence of phosphate ions at the sealer-dentin interface (*dashed line*) in the control dentin. (*F*) A well-defined interfacial band of phosphates (PO_2^-, PO_3^-) in C-HA nanocomplex conditioned dentin. (*G*) A red-green overlay of chitosan fragment ($C_5H_6NO^+$ [*red*]) with calcium (Ca^+ [*green*]) showing the presence of calcium islands in the conditioned dentin in areas lacking chitosan matrix (*yellow arrows*).

(Fig. 1*B*). Ion maps for CN^- (Fig. 1*C*) show low intensity with no signal areas in the control, whereas increased signals are observed in conditioned dentin (Fig. 1*D*). Figure 1*E* shows red-green overlays of chemical ion maps. The presence of PO_3^- and PO_4^- fragments was nonexistent at the interfacial zone in the control sample, whereas a greater intensity of PO_2^- was found. In contrast, the presence of phosphate was noted in well-defined interfacial bands of PO_2^- and PO_3^- in the conditioned dentin (Fig. 1*F*). The PO_4^- map, although less defined, depicted a dense phosphate presence. The distribution of Ca^+ in islands can be noticed from Figure 1*G* in the conditioned dentin.

The results from normalized spectral intensities are shown in Figure 2. Higher intensities for nonspecific (negative polarity) organic fragments of O^-, CN^-, and CNO^- at both ROIs (Fig. 2*A* and *B*) were observed for the conditioned dentin, with the exception of cysteine residue (SH^-), in comparison with the control. OH^- intensity was higher in total dentin of the conditioned group only. The conditioned dentin (Fig. 2*C*–*E*) showed an increased intensity for specific organic fragments of chitosan with negative polarity ($C_2H_4NO^-$ and $C_3H_4NO_2^-$ at both ROIs) and positive polarity ($C_2H_5O_2^+$, $C_2H_6NO^+$, $C_4H_6NO_2^+$, $C_5H_6NO^+$, $C_5H_5O_2^+$ and $C_5H_6NO_2^+$ fragments at interface) compared with the control. $C_2H_4NO^-$ was used as a characteristic marker fragment of the carboxymethyl group to tag chitosan presence. CHO_2^- was noted to be higher at the interface of the conditioned dentin. Other nonspecific organic fragments (NH_4^+, CH_4N^+, and $C_4H_8N^+$) were noted to be higher (Fig. 2*F*) at the interface in the conditioned dentin.

Inorganic fragments of phosphates such as PO_2^-, PO_3^-, and PO_4^- (Fig. 2*G* and *H*) registered higher intensity at the interface and total dentin ROIs in the conditioned group, whereas PO_3^- and PO_4^- fragments were absent in the control. An increased intensity for CaO^+ and $CaOH^+$ (Fig. 2*I*) was noted in the control sample with Ca^+ and all other higher molecular mass fragments ($CaPO_2^+$, $CaPO_3^+$, $CaPO_4^+$ and $Ca_2PO_3^+$) to be greater in intensity in the conditioned dentin (Fig. 2*J*).

Transmission Electron Microscopic Evaluation

Transmission electron microscopic micrographs are shown in Figure 3*A* and *B*. Isolated mineral aggregates as a thin (1 μm) discontinuous layer with denuded collagen matrix are noted in the control (Fig. 3*A*). Fraying of collagen fibril ends as a sign of degradation can also be noted, whereas a consistent interfacial layer with appreciably increased thickness (5 μm) (Fig. 3*B*) and abundant in coarse mineral aggregates encapsulated in a gel-like matrix was observed in the conditioned dentin. The nanometric-sized aggregates were noted deposited in close adaptation to the underlying collagen matrix.

DISCUSSION

In this study, chemical modification at the TCS sealer–dentin interface after conditioning with C-HA nanocomplexes was characterized with monolayer sensitivity. Previously, interfacial characterization for mineral trioxide aggregate (MTA)-based cements has been attempted using scanning electron microscopy coupled with energy-dispersive spectroscopy and electron probe microanalysis, which have limited resolution requiring peak deconvolution such as that reported for phosphorus masking by zirconium peaks[24,25]. Further sample preparation steps, the inability to detect trace elements, and organic materials are other reported disadvantages. Techniques like

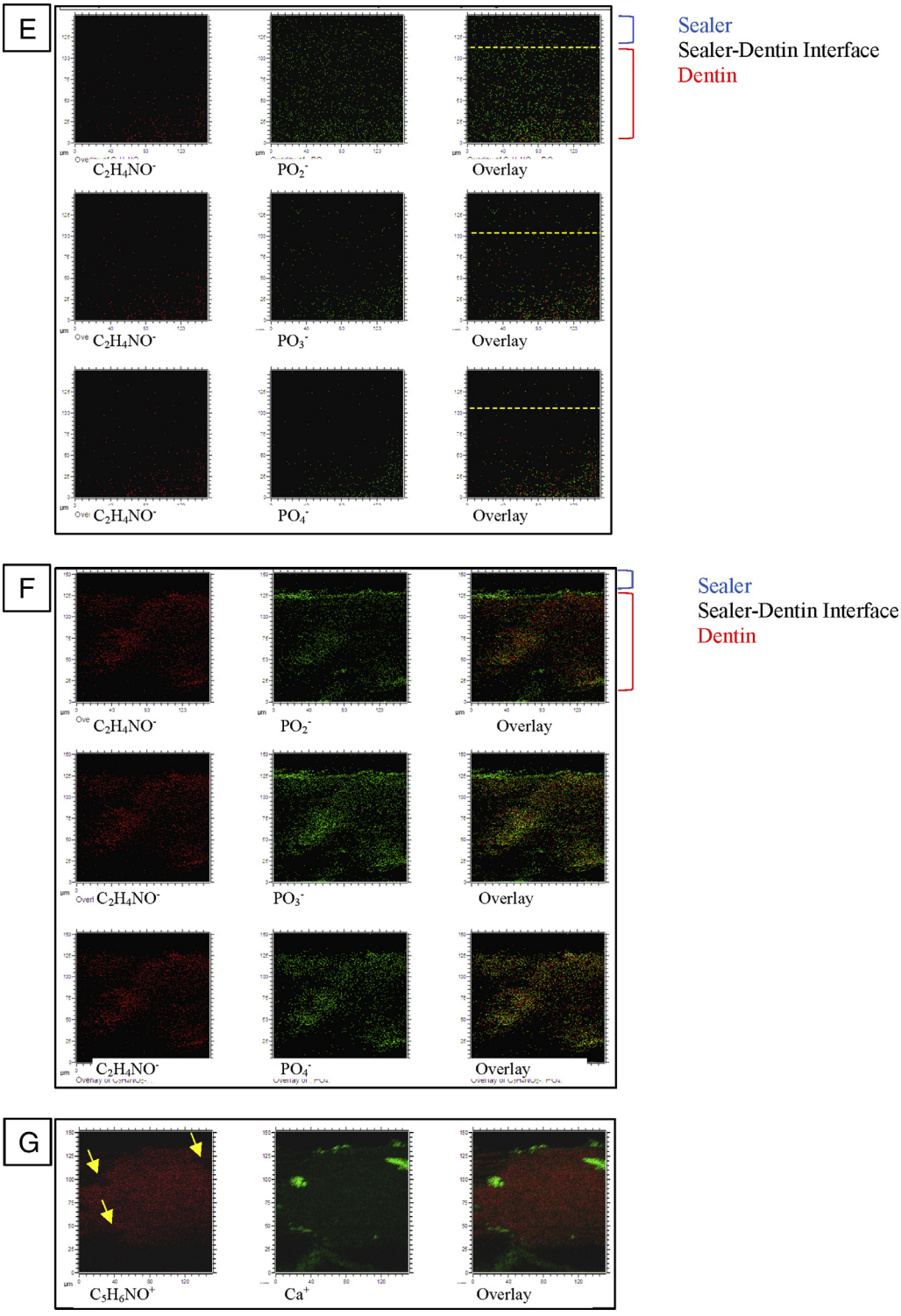

FIGURE 1 – *(Continued)*

confocal laser scanning microscopy are unable to provide chemical information that warrants the use of additional analysis[26]. The use of fluorescent dyes has also been reported; nevertheless, rhodamine is preferentially imbibed by MTA-based materials, causing its movement across the sealer-dentin interface difficult[27]. In addition, the small-sized fluorescein particles are easily taken up by dentin, which further makes the investigations on interfacial gradient difficult[27]. Hence, an advanced high-resolution surface characterization technique was an important prerequisite for interfacial characterization in endodontics.

In TOF-SIMS, a primary ion beam directed onto the sample causes surface ionization (1–2 monolayers)[28]. The time of flight based on molecular mass is then used for fingerprint identification of these secondary ions[29]. Specific advantages for using TOF-SIMS in the current study included its

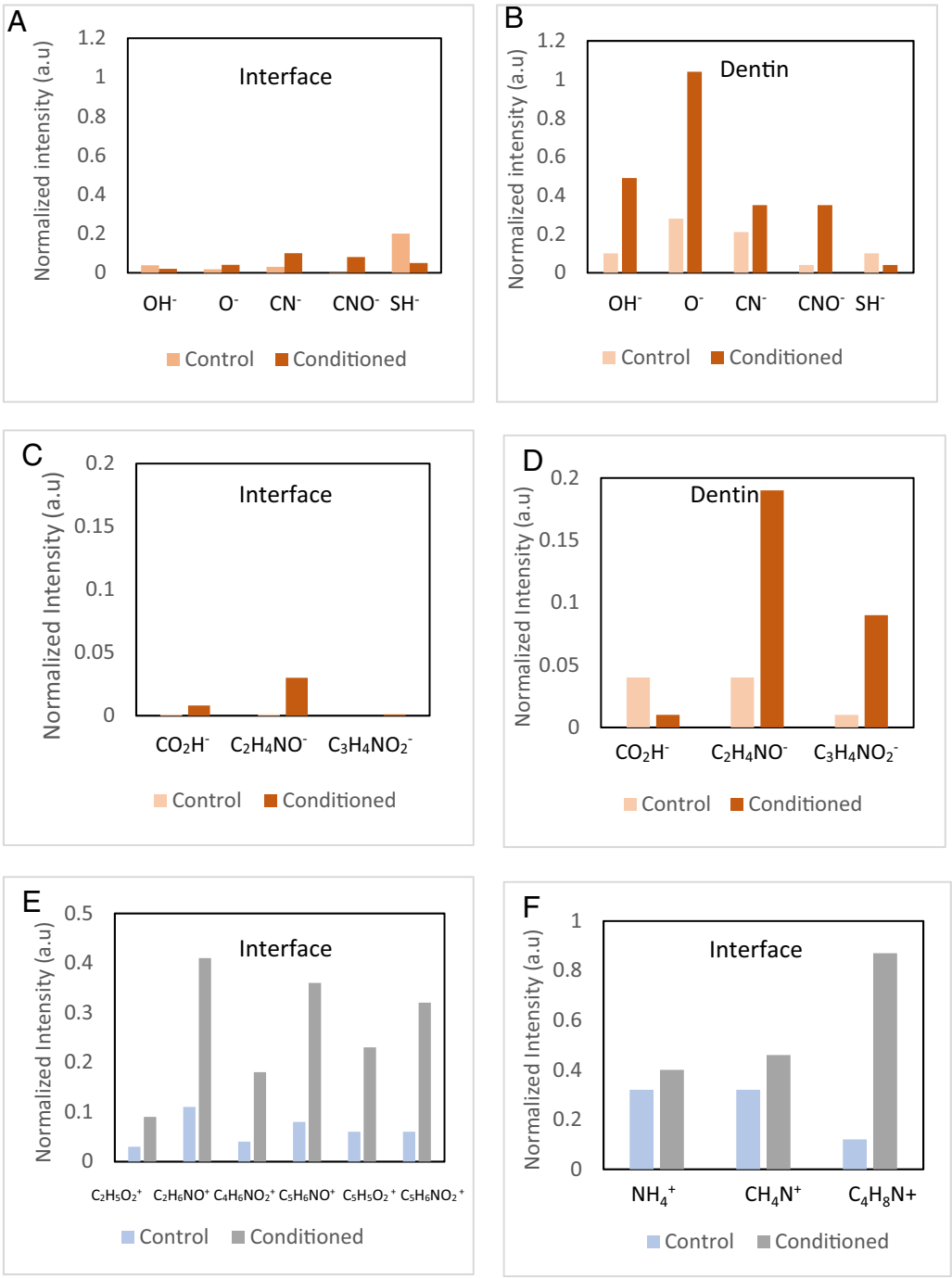

FIGURE 2 – Normalized mass spectral intensities for negative and positive polarity at the interfacial and total dentin ROIs. (*A*) Negative polarity nonspecific protein fragments at the interface and (*B*) total dentin. (*C*) Negative polarity characteristic chitosan fragments at the interface and (*D*) total dentin. (*E*) Positive polarity characteristic chitosan fragments and (*F*) nonspecific organic fragments at the interface. (*G*) Phosphate fragments at the interface and (*H*) total dentin. (*I*) The presence of tricalcium silicate hydration products (Ca^+, CaO^+, and $CaOH^+$) at the interface. (*J*) Higher molecular mass fragments ($CaPO_2^+$, $CaPO_3^+$, $CaPO_4^+$, and $Ca_2PO_3^+$) of calcium phosphates at the interfacial dentin.

sensitivity to identify spatially resolved chemical characteristics of elemental and molecular fragments of the thin modified layer on the conditioned dentin. This is significant because chemical associations provide a far greater understanding of the nature of mineralization[30]. Retrospective analysis granted complete freedom to choose specific areas with precision for analysis. Operating parameters are crucial because they dictate the yield of secondary ions; therefore, the control and conditioned dentin samples were run under the same experimental parameters[31].

One of the major limitations of using TOF-SIMS analysis in biological samples is the difficultly in generating quantitative information for statistical analysis. This is attributed to the high resolution and high sensitivity of the spectra/maps generated by the system and variations associated with different biological samples. Thus, TOF-SIMS is primarily used for qualitative assessments[17–21]. In the current study, qualitative analysis was performed to

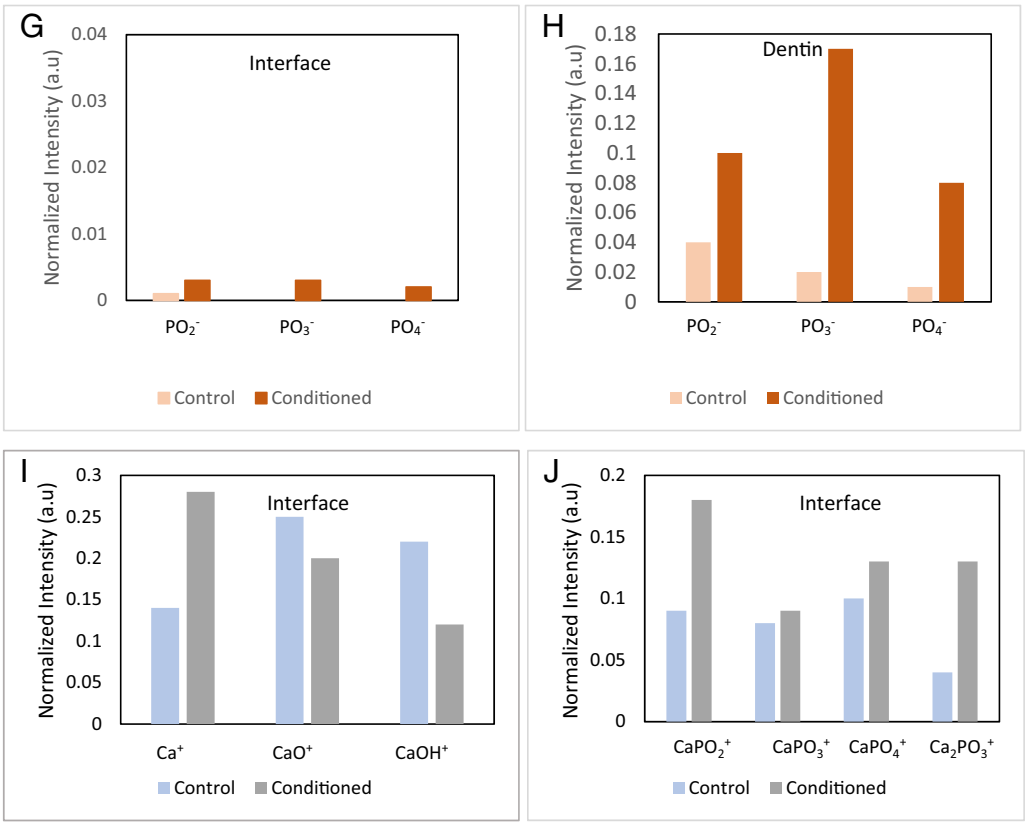

FIGURE 2 – *(Continued)*

examine the interfacial chemical changes and associated trends. The ion maps generated from the TOF-SIMS have 256 × 256 pixels from an average of 20 scans over an area of 150 × 150 μm, which contains more than 65,000 spectra. It is challenging to process these large data sets quantitatively while the smallest spectral changes are considered. Thus, keeping in mind the limitations associated with TOF-SIMS analysis based on small ROIs from a single window of the rastered area along with the limited ion yield of higher mass fragments from nonstandardized biological interfaces, normalized intensities were created for comparison, and statistical analysis was avoided.

The presence of Ca, P, and Si ion-rich deposits along the calcium silicate cement–dentin interface and dentin subsurface to varying depths was reported by previous studies[24,25]. The variation in interfacial layer thickness (4.8–14.5 um) from scanning electron microscopic measurements has been attributed to the decreased length of

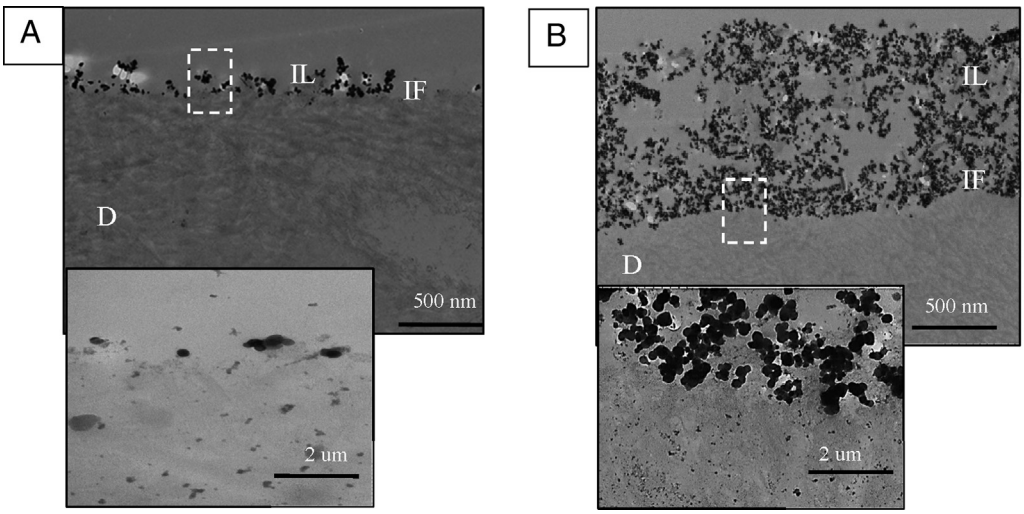

FIGURE 3 – Transmission electron microscopic micrographs showing the sealer-dentin (D) interface (IF) with the presence of an interfacial layer (IL). (*A*) The control dentin shows a thin, discontinuous interfacial layer with collagen fraying. (*B*) The conditioned dentin shows a closely adapted interfacial layer with markedly increased thickness.

interaction between the phosphate from the supersaturated solution and the calcium leached from the calcium silicate cements[12]. Along similar lines, a 5-μm-thick layer was identified on the conditioned dentin from the total ion chemical maps and transmission electron microscopic micrographs. However, it was difficult to measure a consistent layer in the controls.

The presence of phosphate as a well-delineated band in the conditioned dentin group was an important finding in this study. TCS was tested as a calcium source based on the earlier biomineralization studies[10,32]. The presence of a calcium phosphate monobasic phase in the sealer could have been a potential source for phosphate fragments. However, in the control sample, this contribution was very nominal and virtually nonexistent at the interface for PO_3^- and PO_4^- fragments. The same finding was reinforced with a lower registration of calcium phosphate intensities. Similarly, as the TCS hydration continued, more calcium hydroxide ($Ca[OH]_2$) was formed, but because of the limited phosphate availability in the control sample, it remained unused and recorded a higher intensity[9,10]. This is in contrast to earlier studies in which a large quantity of phosphate-based fluid is provided[25]. Such an approach clearly established the source of phosphate to be the C-HA nanocomplexes without any confounding factors.

Demineralized dentin allowed mapping of calcium gradients from the interface into the dentin. Registration of Ca^+ in the conditioned dentin as dense islands may be explained by the lack of chitosan fragment in those areas as is evident on the red-green overlay, whereas in the rest of the image, the Ca^+ signals were masked by the near homogenous presence of chitosan of ~5 μm, which is way larger than the 1 to 2 monolayer sampling depth of TOF-SIMS. Among others, high O^- and OH^- signals were noted in the conditioned sample, which represented substrate signals and were suggestive of calcium phosphate precipitation[30].

An overlap of signals occurred from the dentin matrix and the chitosan layer. Therefore, the chemical nature of the conditioned layer was established through the presence of characteristic positive and negative chitosan fragments along with nonspecific fragments[23,30]. The presence of SH^- as a cysteine residue was identified as an intense signal in the control group in comparison with the conditioned group wherein its presence was almost negligible. Because cysteine residue is not present in the chitosan structure[30], this further supported the adsorption/integration of chitosan as an additional, modified layer at the sealer-dentin interface. Also, the minor SH^- signals in the nanocomplex group may also point at the close adaptation of the modified layer to the underlying dentin.

As reported in an earlier study, the formation of $Ca(OH)_2$ by calcium silicate cement results in caustic etching and degradation of collagen matrix[26]. Such a finding may also be supported by the lack of CN^- signals seen (black zone) in the few microns nearest to the interface in the control sample, whereas strong CN^- signals can be clearly seen emanating from the integration of C-HA nanocomplexes in the conditioned dentin. This is supplemented by transmission electron microscopic images showing collagen fraying, whereas a very homogenous surface is observed in the conditioned dentin, highlighting a potential protective effect on dentin collagen.

TCS-based cements have been reported to interact with dentin through the formation of an ion-rich layer and sealer tags[24]. The use of C-HA nanocomplexes in this study provided a basis for restoring the chemical characteristics of demineralized dentin. This may be explained by the fact that as the TCS continued to set, $Ca(OH)_2$ was produced and underwent hydrolysis to provide a continued supply of calcium and OH^- ions[32]. The hydrophilic nature of carboxymethyl chitosan would have attracted more water molecules close to the C-HA nanocomplexes at the sealer-dentin interface forming a microenvironment, allowing amorphous calcium phosphate dissolution and precipitation[33] that aided in providing a phosphate source. The accumulation of calcium, hydroxyl, and phosphate ions inside the chitosan microenvironment formed the ion-rich layer, which would facilitate subsequent phase transformation toward the thermodynamically stable phase assisted by medium alkalinity[10]. The presence of C-HA nanocomplexes could have also provided added heterogeneous nucleation sites to sequester Ca^+ ions with its carboxyl groups as well and hastened the reaction kinetics.

All biomimetic mineralization schemes are composed of fundamental components requiring organic-inorganic interaction to initiate nucleation and an uninterrupted mineral replenishment source, which was provided by C-HA nanocomplex conditioning of the dentin. By mimicking the role of noncollagenous proteins, the adsorption of C-HA nanocomplexes on dentin collagen could produce a negatively charged surface and therefore reduced interfacial energy between the aqueous microenvironment and dentin, allowing mineral deposition[5]. Because nucleation and growth of minerals is proportional to the concentration of the available ions[34], enhanced bioactivity of TCS was observed with C-HA nanocomplex conditioning, which resulted in a modified interaction between the TCS and dentin as established in the current study.

The findings from this study highlighted the possible contributions of C-HA nanocomplex conditioning in chemically modifying the dentin surface and subsurface by forming an ion-rich layer. This may facilitate enhanced interfacial integrity of sealer-dentin interfaces and improved dentin mechanical integrity in root-filled teeth.

ACKNOWLEDGMENTS

Supported by the Ontario Centres of Excellence (grant number 29388), Canadian Foundation of Innovation-Leading Edge Fund (grant number 30765), and the University of Toronto. The authors would also like to thank Innovative BioCeramix Inc, Vancouver, Canada for graciously supplying iRoot SP sealer for this study.

The authors deny any conflicts of interest related to this study.

REFERENCES

1. Bertassoni L. Dentin on the nanoscale: hierarchical organization, mechanical behavior and bioinspired engineering. Dent Mater 2017;33:637–49.
2. Gu LS, Huang XQ, Griffin B, et al. Primum non nocere - the effects of sodium hypochlorite on dentin as used in endodontics. Acta Biomater 2017;61:144–56.

3. Dogan Buzoglu H, Calt S, Gümüsderelioglu M. Evaluation of the surface free energy on root canal dentine walls treated with chelating agents and NaOCl. Int Endod J 2007;40:18–24.
4. Tartari T, Bachmann L, Maliza AG, et al. Tissue dissolution and modifications in dentin composition by different sodium hypochlorite concentrations. J Appl Oral Sci 2016;24:291–8.
5. Xu Z, Neoh KG, Lin CC, Kishen A. Biomimetic deposition of calcium phosphate minerals on the surface of partially demineralized dentine modified with phosphorylated chitosan. J Biomed Mater Res B Appl Biomater 2011;98:150–9.
6. Topçuoğlu HS, Tuncay Ö, Demirbuga S, et al. The effect of different final irrigant activation techniques on the bond strength of an epoxy resin-based endodontic sealer: a preliminary study. J Endod 2014;40:862–6.
7. Rechenberg DK, Thurnheer T, Zehnder M. Potential systematic error in laboratory experiments on microbial leakage through filled root canals: an experimental study. Int Endod J 2011;44:827–35.
8. Ferrari M, Mason PN, Goracci C, et al. Collagen degradation in endodontically treated teeth after clinical function. J Dent Res 2004;83:414–9.
9. Xuereb M, Vella P, Damidot D, et al. In situ assessment of the setting of tricalcium silicate-based sealers using a dentin pressure model. J Endod 2015;41:111–24.
10. Tay FR, Pashley DH, Rueggeberg FA, et al. Calcium phosphate phase transformation produced by the interaction of the Portland cement component of white mineral trioxide aggregate with a phosphate-containing fluid. J Endod 2007;33:1347–51.
11. Shao C, Zhao R, Jiang S, et al. Citrate improves collagen mineralization via interface wetting: a physicochemical understanding of biomineralization control. Adv Mater 2018;30.
12. Kim JR, Nosrat A, Fouad AF. Interfacial characteristics of Biodentine and MTA with dentine in simulated body fluid. J Dent 2015;43:241–7.
13. Kishen A, Shrestha S, Shrestha A, et al. Characterizing the collagen stabilizing effect of crosslinked chitosan nanoparticles against collagenase degradation. Dent Mater 2016;32:968–77.
14. Hashmi A, Xu Z, Kishen A. Impact of dentin substrate modification with chitosan-hydroxyapatite precursor nanocomplexes on sealer penetration and tensile strength. J Endod 2019;45:935–42.
15. Chen Z, Cao S, Wang H, et al. Biomimetic remineralization of demineralized dentine using scaffold of CMC/ACP nanocomplexes in an in vitro tooth model of deep caries. PLoS One 2015;10:e0116553.
16. Wang Y, Van Manh N, Wang H, et al. Synergistic intrafibrillar/extrafibrillar mineralization of collagen scaffolds based on a biomimetic strategy to promote the regeneration of bone defects. Int J Nanomedicine 2016;11:2053–67.
17. Malmberg P, Nygren H. Methods for the analysis of the composition of bone tissue, with a focus on imaging mass spectrometry (TOF-SIMS). Proteomics 2008;8:3755–62.
18. Gotliv BA, Veis A. Peritubular dentin, a vertebrate apatitic mineralized tissue without collagen: role of a phospholipid-proteolipid complex. Calcif Tissue Int 2007;81:191–205.
19. Eriksson C, Malmberg P, Nygren H. Time-of-flight secondary ion mass spectrometric analysis of the interface between bone and titanium implants. Rapid Commun Mass Spectrom 2008;22:943–9.
20. Gotliv BA, Veis A. The composition of bovine peritubular dentin: matching TOF-SIMS, scanning electron microscopy and biochemical component distributions. New light on peritubular dentin function. Cells Tissues Organs 2009;189:12–9.
21. Kolosowski KP, Sodhi RN, Kishen A, Basrani BR. Qualitative analysis of precipitate formation on the surface and in the tubules of dentin irrigated with sodium hypochlorite and a final rinse of chlorhexidine or QMiX. J Endod 2014;40:2036–40.
22. Chen X, Park H. Chemical characteristics of O-carboxymethyl chitosans related to the preparation conditions. Carbohydrate Polymers 2003;53:355–9.
23. D'Almeida M, Attik N, Amalric J, et al. Chitosan coating as an antibacterial surface for biomedical applications. PLoS One 2017;12:e0189537.
24. Han L, Okiji T. Uptake of calcium and silicon released from calcium silicate-based endodontic materials into root canal dentine. Int Endod J 2011;44:1081–7.
25. Han L, Okiji T. Bioactivity evaluation of three calcium silicate-based endodontic materials. Int Endod J 2013;46:808–14.

26. Atmeh AR, Chong EZ, Richard G, et al. Dentin-cement interfacial interaction: calcium silicates and polyalkenoates. J Dent Res 2012;91:454–9.

27. Camilleri J, Grech L, Galea K, et al. Porosity and root dentine to material interface assessment of calcium silicate-based root-end filling materials. Clin Oral Investig 2014;18:1437–46.

28. Sodhi RN. Time-of-flight secondary ion mass spectrometry (TOF-SIMS):–versatility in chemical and imaging surface analysis. Analyst 2004;129:483–7.

29. Fearn S. An Introduction to Time-of-Flight Secondary Ion Mass Spectrometry (ToF-SIMS) and its Application to Materials Science. San Rafael, CA: Morgan & Claypool Publishers; 2015.

30. Wagener V, Boccaccini AR, Virtanen S. Protein-adsorption and Ca-phosphate formation on chitosan-bioactive glass composite coatings. Appl Surf Sci 2017;416:454–60.

31. Gandolfi MG, Taddei P, Siboni F, et al. Biomimetic remineralization of human dentin using promising innovative calcium-silicate hybrid "smart" materials. Dent Mater 2011;27:1055–69.

32. Prati C, Gandolfi MG. Calcium silicate bioactive cements: biological perspectives and clinical applications. Dent Mater 2015;31:351–70.

33. Yang T, Xiao W, Chen W, Sui L. Effect of carboxymethyl chitosan and aging time on synthesis and storage of amorphous calcium phosphate. J Nanosci Nanotechnol 2016;16:12582–9.

34. Weng J, Liu Q, Wolke JG, et al. Formation and characteristics of the apatite layer on plasma-sprayed hydroxyapatite coatings in simulated body fluid. Biomaterials 1997;18:1027–35.